Molecular Cell, Vol. 7, 387–399, February, 2001, Copyright ©2001 by Cell Press

Solution Structure of ERK2 Binding Domain of MAPK Phosphatase MKP-3: Structural Insights into MKP-3 Activation by ERK2

Amjad Farooq, Gaurav Chaturvedi, Shiraz Mujtaba, Olga Plotnikova, Lei Zeng, Christophe Dhalluin, Robert Ashton, and Ming-Ming Zhou*
Structural Biology Program
Department of Physiology and Biophysics
Mount Sinai School of Medicine
New York University
New York, New York 10029

Summary

MAP kinases (MAPKs), which control mitogenic signal transduction in all eukaryotic organisms, are inactivated by dual specificity MAPK phosphatases (MKPs). MKP-3, a prototypical MKP, achieves substrate specificity through its N-terminal domain binding to the MAPK ERK2, resulting in the activation of its C-terminal phosphatase domain. The solution structure and biochemical analysis of the ERK2 binding (EB) domain of MKP-3 show that regions that are essential for ERK2 binding partly overlap with its sites that interact with the C-terminal catalytic domain, and that these interactions are functionally coupled to the active site residues of MKP-3. Our findings suggest a novel mechanism by which the EB domain binding to ERK2 is transduced to cause a conformational change of the C-terminal catalytic domain, resulting in the enzymatic activation of MKP-3.

Introduction

Regulation of the activity of mitogen-activated protein kinases (MAPKs) has profound biological implications for numerous cellular processes, including neuronal differentiation, mitogenesis, oncogenic transformation, and apoptotic cell death (Cobb and Goldsmith, 1995; Waskiewicz and Cooper, 1995; Kyriakis and Avruch, 1996; Treisman, 1996; Robinson and Cobb, 1997; Lewis et al., 1998). In addition to a host of transcription factors such as c-Jun, c-Fos, Elk-1, and c-Myc, MAPK substrates include membrane-associated and cytoplasmic proteins such as kinases, cytoskeletal elements, phospholipase A_2, and stathmin (Gupta et al., 1995; Karin, 1995; Whitmarsh et al., 1995; Cahill et al., 1996; Treisman, 1996; Wang and Ron, 1996). This diverse set of target proteins illustrates MAPKs' central role in orchestrating many short- and long-term changes in cell function as a result of extracellular stimulation. MAPKs are grouped into three major classes based on their preferential activation by extracellular stimuli and amino acid sequence homology: the extracellular signal-regulated kinase (ERK), the c-Jun N-terminal kinase/stress-activated protein kinase (JNK/SAPK), and p38/RK/CSBP (p38; Cano and Mahadevan, 1995; Gupta et al., 1995, 1996; Marshall, 1995). Stimulation of quiescent cells by hormones, growth factors, cytokines, and environmental stresses leads to rapid phosphorylation and activation of MAPKs. MAPKs are translocated to the nucleus upon activation, where they phosphorylate and activate transcription factors for gene expression. Among early genes that MAPKs induce are genes that encode a family of MAPK phosphatases (MKPs) that dephosphorylate and inactivate MAPKs, thus forming a negative feedback mechanism.

The biological importance of MAPKs is manifested by the tight control of their activity through phosphorylation on two different amino acid residues, namely the threonine and tyrosine residues in a *T*-X-*Y* motif in the activation loop, where X is any amino acid (Ahn et al., 1991; Payne et al., 1991; Robbins et al., 1993). Phosphorylation of both residues is required to maintain high activity (Robbins et al., 1993; Canagarajah et al., 1997). While a considerable amount is known about the activation of MAPKs, a transient and reversible process, the molecular mechanisms of their downregulation are much less understood (Clarke, 1994; Keyse, 1994). Recently, a group of dual specificity MKPs has been shown to exhibit distinct substrate specificity toward MAPKs. For example, MKP-3 and M3-6 (Groom et al., 1996; Muda et al., 1996a, 1996b) are highly selective in inactivating either ERK2 or JNK/SAPK and p38 MAPKs, respectively, whereas PAC1 was discovered by its specific inactivation of ERKs in T cell activation (Rohan et al., 1993; Ward et al., 1994).

All MKPs consist of an N-terminal domain and a C-terminal catalytic domain (Keyse, 1994). Figure 1A shows the organization of functional regions within MKP-3, a prototypic member of the MKP family. The highly conserved C-terminal domains of MKPs contain a tyrosine-specific phosphatase signature sequence *HC*XXXXX*R* at the active site, where cysteine acts as the enzymatic nucleophile and arginine interacts directly with the phosphate group on phosphotyrosine or phosphothreonine (Denu and Dixon, 1995; Tonks and Neel, 1996). A highly conserved aspartic acid also participates in the enzymatic catalysis by acting as a proton donor to the phenolic or hydroxyl oxygen of the leaving group (Stewart et al., 1999; Zhou and Zhang, 1999; Fjeld et al., 2000). On the other hand, the noncatalytic N-terminal domains are divergent among MKPs, and have recently been suggested to be important for substrate specificity. Specifically, Arkinstall and coworkers have shown that inactivation of ERK2 by MKP-3 is highly specific, and that substrate recognition is achieved via direct binding of the N-terminal domain of MKP-3 to ERK2 (Camps et al., 1998; Muda et al., 1998). Interestingly, this interaction results in enhancement of MKP-3 phosphatase activity by ~30-fold (Camps et al., 1998).

Downregulation of MAPK activity through direct association of MKPs is supported by other genetic and biochemical studies. Hyperphosphorylated and thus hyperactivated MAPKs, which are associated with a large fraction of human breast cancers, often contain nonsense mutations that could induce resistance to MKP inactivation (Sivaraman et al., 1997). Further, a gain-of-

*To whom correspondence should be addressed (e-mail: zhoum@inka.mssm.edu).

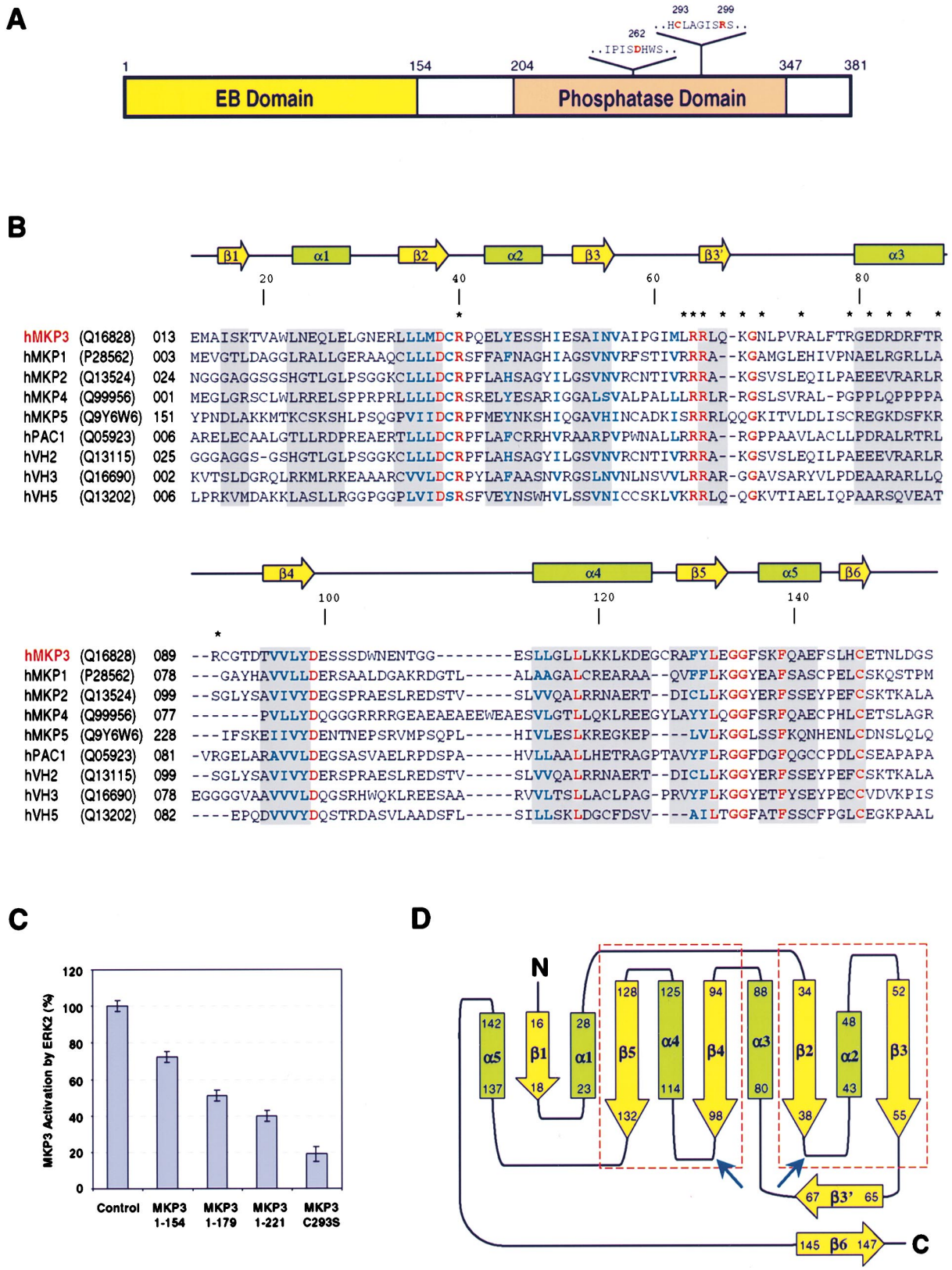

Figure 1. Structural Features of MKP-3 and Sequence Alignment of MKPs

(A) Organization of the MKP-3 polypeptide chain. The N-terminal EB domain used in the structure determination is shown in yellow. The C-terminal catalytic domain is displayed in orange. Numerals indicate residue numbers at the boundaries of various segments. The domain boundaries of the catalytic domain are based on its crystal structure (Stewart et al., 1999). Amino acid sequences surrounding the key active site residues D262, C293, and R299 are depicted.

function mutation of mammalian ERK2 (D319 to asparagine), which does not affect ERK2's basal activity, increases its resistance to MKPs following activation by the MAPK kinase (Brunner et al., 1994; Chu et al., 1996). The resistance of the ERK2 D319N mutant to MKP-3-mediated dephosphorylation has recently been shown to be due to its substantially reduced binding of the phosphatase (Camps et al., 1998). These studies strongly suggest that the physical association of MAPKs and MKPs as well as the MAPK substrate–induced MKP activation provides a critical regulatory mechanism that enables the two proteins to keep each other in check, and thereby guarantees the fidelity of signal transduction.

In an effort to understand the detailed molecular mechanism of ERK2 inactivation by MKP-3, we have determined the high-resolution solution structure of the N-terminal ERK2 binding (EB) domain of MKP-3. Structural and biochemical analyses were used to investigate the EB domain interactions with ERK2 and the catalytic domain, and to gain novel insights into the ERK2-induced enzymatic activation mechanism of MKP-3.

Results and Discussion

Structure Determination

To identify a suitable EB domain construct for structural analysis (Figure 1B), we characterized a series of MKP-3 N-terminal fragments with nuclear magnetic resonance (NMR) spectroscopy and biochemical binding assays. Specifically, overall domain foldedness and structural features of the N- and C-terminal boundaries of the MKP-3 protein of various constructs were assessed based on chemical shift dispersion of backbone amide resonances in two-dimensional (2D) ^{15}N heteronuclear single quantum coherence (HSQC) spectra. These MKP-3 proteins were further analyzed for ERK2 binding by a GST pulldown or enzymatic assay. In the latter experiment, the N-terminal fragments competed with the full-length MKP-3 in the ERK2 binding, resulting in the reduction of enzymatic activation of MKP-3 (Figure 1C). The phosphatase activity of MKP-3 in the presence of ERK2 and a specific N-terminal MKP-3 protein can be measured as *p*-nitrophenyl phosphate (*p*NPP) hydrolysis, monitored by absorbance at 405 nm. From these studies, a fragment consisting of residues 1–154 in MKP-3 was defined as the minimal EB domain, which contains conserved sequences in the MKP family (Figure 1B).

For NMR structural studies, various isotopically (^{2}H, ^{13}C, and ^{15}N) labeled protein samples of the MKP-3 EB domain were overexpressed in bacteria and purified to homogeneity, as described in Experimental Procedures. The backbone and side chain resonances of the protein were assigned from standard heteronuclear three-dimensional triple resonance NMR spectra (Sattler et al., 1999). The structure of the EB domain of MKP-3 was determined from a total of 2540 NMR-derived distance and torsional angle restraints. Figure 2A depicts the backbone atoms (N, C^{α}, and C′) of 20 low-energy structures that were derived from the NMR experimental data. All structures exhibit good geometry, with no violations of distance restraints greater than 0.5 Å, and no dihedral angle violations larger than 5° (Table 1). The atomic root-mean-square (rms) deviations about the mean coordinate position of the backbone and all heavy atoms for the protein residues 10–152 are 0.79 ± 0.12 Å and 1.29 ± 0.12 Å, respectively. Except for a few terminal residues, the overall structures are well defined (Table 1).

Structure Overview

The MKP-3 EB domain consists of an open twisted five-stranded β sheet surrounded by α helices (α1-α5) on both sides, characteristic of a classic Rossmann fold (Figures 2B and 2C). Particularly, two right-handed β-α-β motifs (β2-α2-β3 and β4-α4-β5), which are the most conserved parts of the protein, are joined together with β1 into a five-stranded parallel β sheet, giving an overall strand-folding topology of +3x, +1x, −2x, and −1x (Figure 1C). Additionally, a two-stranded small antiparallel β sheet is formed between β3′, a region connecting β3 and α3 with β6, the C-terminal region of the protein. The two β sheets (β1-β5-β4-β2-β3 and β3′-β6) are oriented nearly perpendicular to each other. The conservation of amino acid sequences implies a similar α/β twisted open sheet structure for the N-terminal domains of the large family of MKPs (Figure 1B).

This open β sheet structure of the conserved Rossmann fold, which is frequently seen in many enzymes, has a variety of folding topologies. The two β strands joined by a crossover connection such as in the β-α-β motif need not be adjacent in the β sheet, and there can also be antiparallel β strands joined with the central parallel β strands (Richardson, 1981). Despite such variations, positions of enzymatic active sites can often be predicted to reside at topological switch points in the α/β structures, where connections from the carboxyl ends of two adjacent β strands go in opposite directions. In a structure such as that of the MKP-3 EB domain, functional residues would then be predicted to be located in the β2-α2 or β4-α4 loop regions (Figure 1C). This prediction is correct for the cell cycle control phosphatase CDC25A that adopts a similar α/β structure, in which a phosphatase signature sequence *HC*XXXXX*R*

(B) Structure-based sequence homology alignment of the N-terminal domains of MKPs. Accession numbers of the proteins are indicated along with the protein sequences. Secondary structure assignments from our MKP-3 EB domain structure are shown as colored rectangles (α helices) and arrows (β strands) above the aligned sequences. Asterisks highlight residues in the MKP-3 protein that were subjected to site-directed mutagenesis. Absolutely or highly conserved residues among the N-terminal domains of MKPs are shown in red and blue, respectively.
(C) Binding of the linker sequence to ERK2. ERK2-induced activation of MKP-3 phosphatase activity was measured as *p*NPP hydrolysis with or without the MKP-3 C293S mutant or the various N-terminal fragments of MKP-3 that contain the EB domain and linker sequences of different lengths (see Experimental Procedures). Data for the enzymatic activity measurements represent an average of three independent experiments.
(D) Topology of the EB domain of MKP-3. Strands and helices are represented by arrows (yellow) and cylinders (green), respectively. Numerals indicate residue numbers at the boundaries of secondary structural elements. The two right-handed β-α-β motifs are boxed in dashed lines (red), and the β2-α2 and β4-α4 loops representing topological switch points in a Rossmann fold are indicated by arrows.

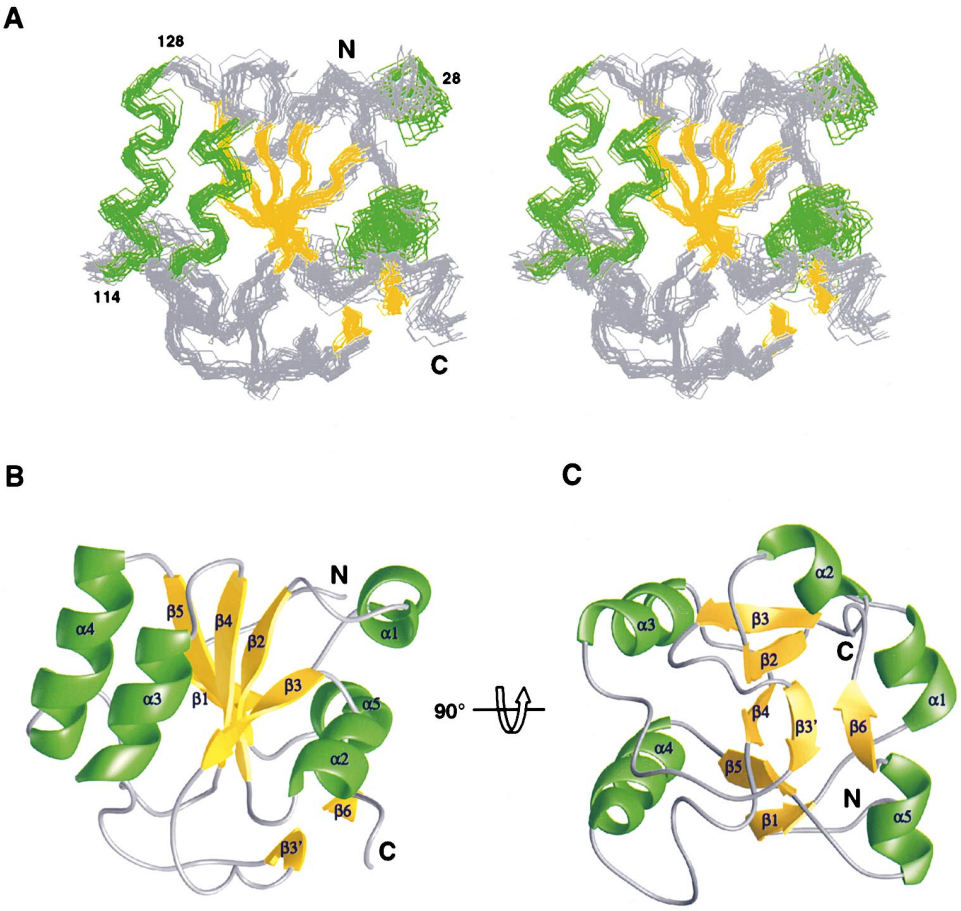

Figure 2. Overview of the MKP-3 EB Domain Structure

(A) Stereoview of the backbone atoms (N, C^{α}, and C′) of 20 superimposed NMR-derived structures of the MKP-3 EB domain (residues 10–152). The terminal residues, which are structurally disordered, are omitted for clarity. The secondary structural elements of α helices and β strands are colored in green and orange, respectively. These figures were produced using InsightII.

(B) Ribbon depiction of the averaged minimized NMR structure of the EB domain. The orientation of the protein structure in (B) is as shown in (A). The color-coding scheme for α helices and β strands is the same as that used in (A).

(C) Ribbon diagram of the EB domain structure, rotated ~90° from the orientation in (B) as indicated in the figure. These figures were prepared using Ribbons (Carson, 1991).

is located precisely in the region between β4 and α4. This 8-residue enzymatic sequence in CDC25A is replaced by an unrelated 15-residue sequence in MKP-3 (residues 99–113).

ERK2 Binding and Mutagenesis

To test whether this 15-residue β4-α4 loop in MKP-3 is important for its binding to ERK2, we performed NMR titration of the EB domain (18 kDa) with ERK2 (42 kDa). Phosphorylation of ERK2, which is important for nuclear localization of ERK2 in cells, has been shown to promote its protein dimerization (Khokhlatchev et al., 1997; Cobb and Goldsmith, 2000). The dissociation constants (K_D) for homodimerization of the phosphorylated or unphosphorylated ERK2 were reported to be about 7.5 nM and 20 μM, respectively (Khokhlatchev et al., 1997). Thus, at the protein concentration of ~0.3 mM in our NMR study, ERK2 exists as a homodimer. The complex of the MKP-3 EB domain and ERK2 is therefore ~120 kDa, which poses a challenging task for the NMR study. To facilitate characterization of MKP-3 binding to ERK2, we employed a recently developed NMR technique of 2D ^{15}N-edited transverse relaxation-optimized spectroscopy (TROSY; Pervushin et al., 1997, 1998), with a uniformly ^{15}N/^{2}H-labeled EB domain and unlabeled ERK2. A representative region of the ^{15}N-TROSY spectra is depicted in Figure 3A, where backbone amide signals of some MKP-3 residues showed ligand concentration-dependent chemical shift changes and line broadening upon ERK2 binding. These perturbations are likely to be due to the formation of a more slowly tumbling complex and chemical exchange. The latter effect is consistent with the protein–protein interaction ($K_D < 5$ μM) in a slow-to-intermediate exchange on the NMR timescale. Surprisingly, the residues that exhibited major chemical shift perturbations upon ERK2 binding were located on one side of the molecule largely in a region connecting β3 and α3, rather than in the predicted β2-α2 or β4-α4 loop (Figures 3B and 3C). The MKP-3 EB domain binding to ERK2 was not dependent upon ERK2 phosphorylation in our NMR titration experiments, consistent with the

Table 1. NMR Structural Statistics of the EB Domain of MKP-3

Total experimental restraints		2540	
NOE distance restraints		2430	
Manually assigned		1903	
ARIA assigned		443	
Total ambiguous		84	
Total unambiguous		2346	
Intraresidue		1113	
Interresidue			
Sequential	($\|i–j\| = 1$)	509	
Medium			
	(i, i + 2)	105	
	(i, i + 3)	115	
	(i, i + 4)	63	
Long range	($\|i–j\| > 4$)	441	
Hydrogen bond restraints		80	
Dihedral angle restraints		30	
Final energies (kcal mol^{-1})			
E_{TOT}		285.2 ± 21.5	
E_{NOE}		83.3 ± 11.5	
E_{DIH}		0.2 ± 0.2	
E_{LJ}[a]		−683.1 ± 27.9	
Cartesian coordinate RMSDs (Å)[b]		N, C^{α}, and C′	all heavy atoms
Residues 10–152		0.79 ± 0.12	1.29 ± 0.12

[a] The Lennard-Jones potential was not used during any refinement stage.
[b] None of these final structures exhibit NOE-derived distance restraint violations greater than 0.5 Å or dihedral angle restraint violations greater than 5°.

previous study of MKP-3 and ERK2 binding with a GST pulldown assay (Camps et al., 1998).

To confirm the ERK2 binding sites on the MKP-3 EB domain, we performed an NMR titration of the EB domain with a peptide derived from ERK2 containing residue D319 (EQYYDPS*D*EPIAEA), which when substituted by asparagine constitutes a gain-of-function phenotype known as the sevenmaker mutant (Brunner et al., 1994; Chu et al., 1996). The EB domain residues that showed major chemical shift changes upon binding to the ERK2 peptide are a subset of those residues identified upon full-length ERK2 binding (Figures 3B), indicating that the D319-containing sequence is indeed directly involved in MKP-3 binding. The affinity of the peptide binding to the EB domain ($K_D > 200$ μM) is much weaker than that of the full-length ERK2 ($K_D < 5$ μM); substitution of asparagine for D319 caused a noticeable reduction in affinity. These data suggest that in addition to D319, other sites in ERK2 are also involved in interactions with the EB domain, thus providing specificity for MKP-3 and ERK2 recognition. These results agree with the observations that this ERK2 D319N mutant can be activated upon phosphorylation by the upstream MAPK kinase and has normal MAPK activity, but is resistant to inactivation by MKPs (Brunner et al., 1994). Collectively, these results strongly argue that functionally important residues in the MKP-3 EB domain are structurally unique, and are located in a region removed from the conserved topological crevices commonly used as enzyme active sites in the α/β structures.

The side of the EB domain molecule containing the β3-α3 region (residues 56–89) is highly positively charged, comprising 8 of 11 arginine residues in the protein (Figures 1B and 5A). This marked structural feature agrees with our observation that MKP-3 binding to ERK2 is sensitive to the ionic strength of the buffer, suggesting that electrostatic interactions are critical in protein binding. To identify key MKP-3 residues for ERK2 association, we used site-directed mutagenesis to alter the arginine residues in this region to alanine, and mutated the other residues that displayed significant NMR resonance perturbations upon ERK2 binding (Figure 3D). The resulting mutants of MKP-3 were analyzed for ERK2 binding with GST pulldown assays. While mutation of most of the selected residues to alanine did not significantly affect protein interactions, substitution of L63, R64, or R65 by alanine completely eliminated EB domain binding to ERK2 (Figure 3E). The importance of these two arginine residues of MKP-3 for ERK2 binding has also been implicated in a recent study (Tanoue et al., 2000).

Notably, a significant portion (40%) of this β3-α3 region (residues 56–79) consists of bulky hydrophobic and aromatic amino acids, namely, I58, I61, M62, L63, L66, L71, V73, L76, and F77 (Figure 1B). Almost all of these residues participate in the formation of a hydrophobic core between this segment and the central β sheet, resulting in a well-defined loop conformation in the structure. On the contrary, L63, like the other two functionally important residues R64 and R65, is exposed to solvent; its mutation to alanine did not significantly affect the loop conformation, as supported by NMR spectral comparison to the wild type. These results imply that in addition to electrostatic interactions involving R64 and R65, hydrophobic contacts are also critical for MKP-3 binding to ERK2. Interestingly, the absolutely conserved residues in the N-terminal domains of various MKPs are localized on the side of the EB domain molecule that also hosts residues important in ERK2 binding (Figure 1B), suggesting a possible similarity in structure or function. However, local conformation of the functionally important β3-α3 region may be quite different, due to

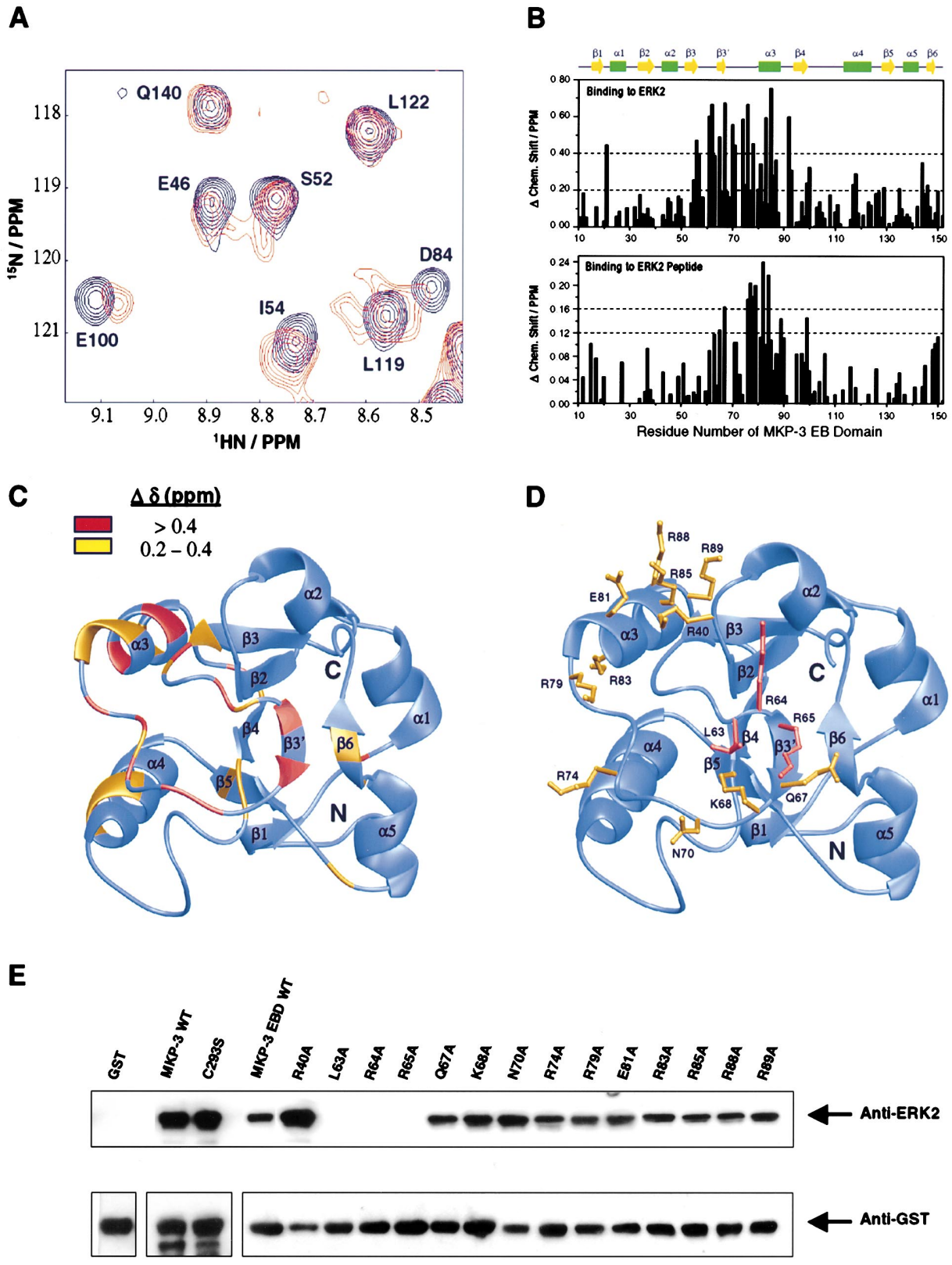

Figure 3. ERK2 Recognition by the EB Domain of MKP-3

(A) Superposition of a representative region of the two-dimensional ^{15}N-TROSY spectra of the MKP-3 EB domain in the free (black) and ERK2-bound form (red).

(B) Plots showing backbone amide chemical shift changes of the amino acid residues of the MKP-3 EB domain upon binding to the full-length

the high degree of variation in the protein sequences. In addition to the highly conserved G69, the β3-α3 sequence of MKP-3 also contains nonconserved residues P59, G60, and P72, which together with the hydrophobic and aromatic residues form a well-ordered conformation in the protein. These structural differences may explain how another member of the MKP family, MKP-4, is nonselectively activated by ERK2, JNK/SAPK, or p38 MAPKs (Camps et al., 1998).

Functional Coupling Between N- and C-Terminal Domains

How does ERK2 binding of the EB domain stimulate MKP-3 phosphatase activity? Our new structure of the EB domain provides insights into the activation mechanism. Notably, the C-terminal segment of the EB domain (residues 145–147) tethers to the other ERK2 binding sites with an antiparallel β sheet involving R65, L66, and Q67 (Figure 1D), as supported by cross-stranded backbone and side chain NOEs. These residues in the C-terminal segment also displayed chemical shift perturbations upon ERK2 binding. In addition, in our ERK2 binding study, the EB domain constructs that contain the linker sequence between the N- and C-terminal domains exhibited higher binding affinity than that of the minimal EB domain in the order of 1–381 > 1–221 > 1–179 > 1–154 (Figure 1C), suggesting that the linker sequence is also involved in ERK2 binding. While the linker sequence is not a part of the EB domain as supported by the NMR data, its functional coupling to the EB domain in ERK2 binding may constitute a key component in the substrate-induced activation mechanism for MKP-3.

To understand how the N-terminal EB domain interacts with the C-terminal catalytic domain in MKP-3, we performed NMR binding studies of these two protein domains. We used the catalytic domain from the MKP PAC1 in the NMR titration to take advantage of its three-dimensional solution structure that we have recently determined (G. C. and M.-M. Z., unpublished data). Consistent with their high sequence homology (51% identity plus 19% similarity), the NMR structure of the PAC1 catalytic domain is very similar to the crystal structure of the catalytic domain of Pyst1 (MKP-3; Stewart et al., 1999), suggesting that these two proteins are closely related in structure and function. Specifically, we added an unlabeled PAC1 catalytic domain to a ~0.5 mM ^{15}N-labeled MKP-3 EB domain and monitored the titration with a series of 2D ^{15}N-HSQC spectra. The interactions between the N- and C-terminal domains were specific, but much weaker (K_D ~100 μM) than that of the EB domain binding to ERK2 (K_D < 5 μM). The former binding is likely to be much stronger in the full-length MKP-3 due to intramolecular interactions. The NMR titration study showed that the residues exhibiting major resonance shifts are situated on the side of the molecule containing the β3-α3 region as well as the C-terminal α5, which partly overlaps with the regions for ERK2 binding (Figures 3C and 4B). These results imply that the EB domain utilizes overlapping regions for interactions with either its C-terminal catalytic domain or ERK2, and that ERK2 binding can alter the interactions between the N- and C-terminal domains of MKP-3.

To further understand how the EB domain interaction with the catalytic domain affects the enzymatic activity of MKP-3, we performed an NMR titration of the ^{15}N-labeled PAC1 catalytic domain with the unlabeled MKP-3 EB domain. The PAC1 catalytic domain contains a compact α/β structure consisting of a central five-stranded mixed β sheet with a folding topology of +2x, +2x, −1x, and −2x, which is sandwiched by four α helices on one side and one helix on the other (Figures 4D and 4E). The conserved phosphatase active site sequence *HCXXXXXR* is located in the β5-α3 loop; the catalytically important D226 (equivalent to D262 in MKP-3) resides in the β4-α2 loop. The NMR titration results show that the residues that underwent major chemical shift perturbations upon EB domain binding are located in proximity to the active site as well as at the C-terminal end of the enzyme. Unlike the EB domain, the majority of the most significantly perturbed residues in the catalytic domain are located in the loops that connect the secondary structural elements. Because it contains a cluster of amino acid residues affected by EB domain binding, the region comprising the C-terminal ends of α4 and α5 is possibly one of the key contact points for the EB domain association. It is important to note that in the NMR structure of the PAC1 catalytic domain, the α4-α5 loop is closely packed against the β5-α3 loop that contains the active site sequence. This structural feature agrees with a hydrogen bond observed between the N and Nδ2 atoms of N333 in the α4-α5 loop and the Oγ atom of S298 of the active site sequence in the crystal structure of the MKP-3 catalytic domain (Stewart et al., 1999). The functional importance of this cross-loop interaction is under-

ERK2 (molar ratio 1:1, upper panel) and the ERK2 peptide containing D319 (molar ratio 1:3, lower panel). The results reflect the sum of the chemical shift changes (Δδ) of the backbone amide ^{1}H and ^{15}N resonances upon binding to either the ERK2 protein or peptide, as observed in the two-dimensional ^{15}N-TROSY and ^{15}N-HSQC spectra, respectively. The dashed lines indicate categorization of the extent of chemical shift perturbations used in ribbon depiction in (C). The secondary structural elements of β strands (yellow arrows) and α helices (green cylinders) of the EB domain are shown along the protein sequence at the top of the plot.

(C) Ribbon representation of the EB domain showing amino acid residues that underwent backbone amide resonance changes upon ERK2 binding. Residues of the protein are categorized into three groups according to the extent of their chemical shift perturbation, as indicated by the dashed lines in (B). These amino acid residues are color coded: red, large resonance shifts (≥0.40 ppm); gold, medium changes (<0.40 and ≥0.20 ppm); and blue, small or no changes (<0.20 ppm).

(D) Ribbon diagram of the EB domain depicting side chains of the amino acid residues that were subjected to site-directed mutagenesis. The three residues L63, R64, and R65 that are essential for ERK2 binding are shown in red, whereas the other residues are in yellow.

(E) Effects of point mutations of the MKP-3 EB domain on interactions with ERK2, determined by using a GST pulldown assay as described in Experimental Procedures. Western blots show the amounts of protein in the binding assay and the extent of interactions of MKP-3 proteins with ERK2. The various MKP-3 proteins used in this binding study include GST-fusion proteins of the wild-type and active site C293S mutant of the full-length MKP-3, as well as the wild-type and mutants of the N-terminal EB domain of MKP-3.

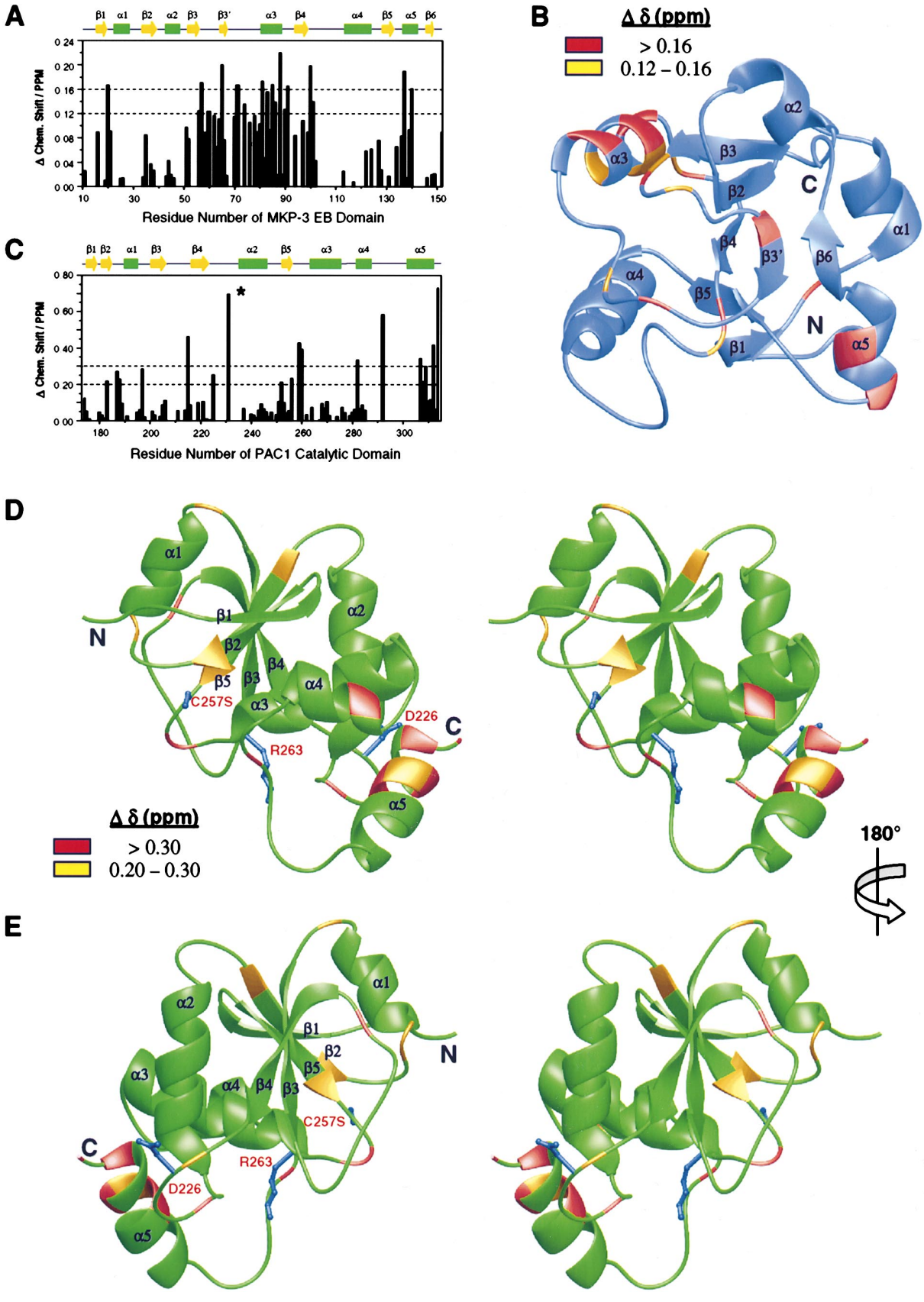
A
β1 α1 β2 α2 β3 β3' α3 β4 α4 β5 α5 β6
Δ Chem. Shift / PPM
Residue Number of MKP-3 EB Domain
B
Δ δ (ppm)
> 0.16
0.12 – 0.16
α2
α3
β3
β2
C
α1
β4
β3'
β6
α4
β5
N
β1
α5
C
β1 β2 α1 β3 β4 α2 β5 α3 α4 α5
Δ Chem. Shift / PPM
Residue Number of PAC1 Catalytic Domain
D
α1
β1
α2
N
β2
β4
β5
β3
α4
C257S
α3
D226
C
R263
α5
Δ δ (ppm)
> 0.30
0.20 – 0.30
180°
E
α1
α2
β1
β2
N
α3
β5
α4
β4
β3
C257S
C
R263
D226
α5

lined by the observation that the mutation of the several conserved residues in the α4-α5 loop (SPNF; residues 331–334) to alanine resulted in a total loss of MKP-3 activation by ERK2 (Stewart et al., 1999). Together, these data strongly suggest that alteration of interactions between the EB and catalytic domains due to ERK2 binding can allosterically trigger conformational change of the latter protein, resulting in a spatial reconfiguration of residues at the enzymatic active site.

A Model for MKP-3 Activation

The surface of the MKP-3 EB domain molecule is electrostatically polarized (Figure 5A). The positively and negatively charged residues are clustered on opposite sides of the protein. The highly positive cluster consisting of a majority of arginine residues in the protein resides around the regions where many amino acid residues underwent NMR resonance perturbations upon ERK2 binding (Figures 3C and 5A). Similarly, ERK2 also has a unique electrostatic surface distribution. A highly negatively charged region containing D319, which is important for MKP-3 binding, is situated opposite a positively charged side that hosts the enzymatic activation loop containing phosphotyrosine and phosphothreonine (Figure 5B). These distinct electrostatic properties of two clusters of oppositely charged residues on the two proteins suggest that the interaction between the MKP-3 EB domain and ERK2 is driven by electrostatic forces. While the negatively charged region containing D319 in ERK2 was implicated to be a conserved docking site in MAPKs common to substrates, activators, and regulators (Tanoue et al., 2000), our NMR titration studies of the EB domain with the full-length ERK2 or the D319-containing ERK2 peptide suggest that other parts of ERK2 also contribute to MKP-3 recognition. Together, these interactions determine binding specificity between ERK2 and MKP-3.

The ERK2-induced enzymatic activation of MKP-3 requires its N-terminal EB domain. The catalytic domain alone (without the EB domain) has very low phosphatase activity, comparable to that of the full-length MKP-3 in the absence of ERK2, and it cannot be activated by ERK2 (Camps et al., 1998; A. F. and M.-M. Z., unpublished data). These observations argue that the role of the EB domain is not simply to suppress the enzymatic activity of MKP-3, and suggest that the intimate coupling between the N- and C-terminal domains is required for an allosteric effect on the active site conformation of MKP-3.

The need for such an allosteric effect was hinted at by the crystal structure of the MKP-3 catalytic domain (Stewart et al., 1999). On the basis of enzyme kinetics and mutational analyses of MKP-3, it was suggested that D262 is required for enzymatic catalysis by acting as a proton donor to the phenolic or hydroxyl oxygen of the leaving group (Stewart et al., 1999; Zhou and Zhang, 1999; Fjeld et al., 2000). In the structure of the MKP-3 catalytic domain, this enzymatically critical residue located in a loop, however, is nearly 10 Å away from the nucleophilic cysteine and arginine at the active site, suggesting that the loop must undergo conformational rearrangement in the activated enzyme. The disengagement of D226 in PAC1 (equivalent to D262 in MKP-3) from the other enzymatic active site residues is also observed in the NMR structure of the catalytic domain (Figures 4D and 4E). E231 (highlighted by an asterisk in Figure 4C), which is one of the most significantly perturbed residues upon EB domain binding, is located in the β4-α2 loop that hosts D226. Residue E225 in the same loop also showed significant chemical shift change. Furthermore, α4 and α5, which have been suggested to be key contact sites for EB domain association based on our NMR titration results, are located in proximity to the β4-α2 loop. These observations suggest that the EB domain binding to ERK2 can affect its association with the catalytic domain, which in turn triggers the β4-α2 loop to undergo a rigid body rotation hinging on the backbone atoms of E225 and E231, thus positioning

Figure 4. Interactions between the EB Domain and the Catalytic Domain

(A) A plot depicting backbone amide chemical shift changes of the MKP-3 EB domain residues upon binding to the catalytic domain of PAC1 (molar ratio 1:2). The results reflect the sum of the chemical shift changes (Δδ) of the backbone amide ^{1}H and ^{15}N resonances upon binding to the catalytic domain, as observed in the 2D ^{15}N-HSQC spectra. The dashed lines indicate categorization of the extent of chemical shift perturbations used in ribbon depiction in (C). The secondary structural elements of β strands (yellow arrows) and α helices (green cylinders) of the EB domain are shown along the protein sequence at the top of the plot.

(B) Ribbon diagram of the N-terminal EB domain of MKP-3 illustrating amino acid residues that underwent chemical shift perturbations upon addition of the C-terminal catalytic domain of the MKP PAC1, as observed in the NMR titration experiment. Residues of the protein are categorized into three groups according to the extent of their chemical shift perturbation, as indicated by the dashed lines shown in (A). The residues are color coded: red, large resonance shifts (≥0.16 ppm); gold, medium changes (<0.16 and ≥0.12 ppm); and blue, small or no changes (<0.12 ppm).

(C) A plot showing backbone amide chemical shift changes of amino acid residues of the PAC1 catalytic domain upon binding to the MKP-3 EB domain (molar ratio 1:2). An asterisk marks residue E231 in the β4-α2 loop that also contains D226. The results reflect the sum of the chemical shift changes (Δδ) of the backbone amide ^{1}H and ^{15}N resonances of the PAC1 catalytic domain upon binding to the corresponding protein, as observed in the 2D ^{15}N-HSQC spectra. The dashed lines indicate classification of the extent of chemical shift perturbation used in ribbon depictions in (D) and (E). The secondary structural elements of β strands (yellow arrows) and α helices (green cylinders) of the PAC1 catalytic domain are shown along the protein sequence at the top of the plot.

(D) Ribbon stereoview of the structure of the C-terminal catalytic domain of the MKP PAC1, illustrating residues that underwent chemical shift perturbations upon addition of the N-terminal EB domain of MKP-3. Residues of the protein are classified as three groups according to the extent of chemical shift perturbations, as indicated by the dashed lines shown in (C). The corresponding residues are color coded: red, large resonance shifts (≥0.30 ppm); gold, medium changes (<0.30 and ≥0.20 ppm); and blue, small or no changes (<0.20 ppm). Side chains of the key amino acid residues at the enzymatic active site are depicted in blue, namely, D226, C257S, and R263. Note that the enzymatic nucleophile C257 was changed to serine in the PAC1 catalytic domain for the NMR structural analysis.

(E) Ribbon stereoview showing another side of the structure of the C-terminal catalytic domain of the MKP PAC1, rotated ~180° from the orientation in (D), as indicated in the figure.

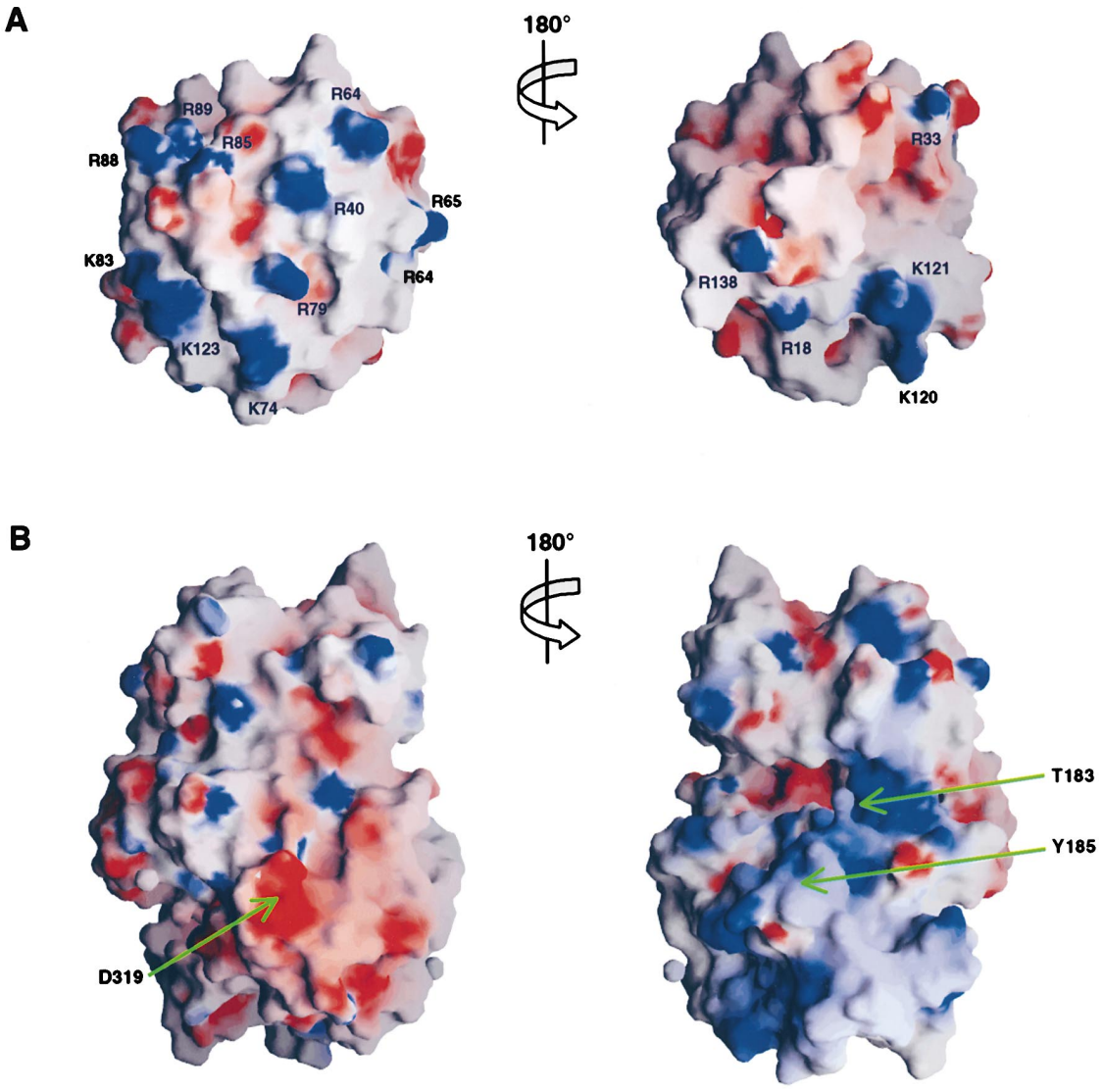

Figure 5. Electrostatic Potential Surface Representations of the MKP-3 EB Domain and ERK2

(A) Electrostatic potential map of the MKP-3 EB domain. Negatively and positively charged residues are shown in red and blue, respectively. Orientation of the molecular surface representation is shown in Figure 3C, rotated clockwise by ~60° about the vertical axis. Numerals indicate specific amino acid residues of the protein.

(B) Electrostatic potential map of ERK2. Negatively and positively charged residues are shown in red and blue, respectively. Numerals indicate locations of functionally important amino acid residues of the protein, including D319 as well as T183 and Y185 in the activation loop.

D226 to be closer to the other key active site residues. Together, these data demonstrate that the enzymatic activity of MKP-3 is controlled by a mechanism of substrate-induced activation rather than autoinhibition.

The central role of the EB domain in controlling ERK2 recognition and enzymatic activation of MKP-3 is illustrated in a model for the substrate-induced MKP-3 activation shown in Figure 6. Upon dual phosphorylation by an upstream MAPK kinase, ERK2 becomes activated and forms a homodimer. Due to disengagement of its active site residues, upon expression, MKP-3 exists in a conformation that is not optimal for enzymatic catalysis (low-activity state). Binding of the EB domain and its following linker sequence to the phosphorylated and activated ERK2 alters their interactions with the catalytic domain. This conformational effect, along with the catalytic domain binding to ERK2, allosterically triggers the MKP-3 active site residues to reconfigure to an enzymatically active conformation (high-activity state), thereby facilitating the catalysis of dual dephosphorylation and inactivation of ERK2.

Conclusions

Almost all of the known protein tyrosine-specific phosphatases and dual specificity tyrosine/threonine phosphatases contain a highly conserved sequence *HC*XXXXX*R* at enzymatic active sites, and possibly possess very similar catalytic mechanisms. Thus, it is clear that distinct regulatory mechanisms must have evolved to control their activities. Comparison of regulatory mecha-

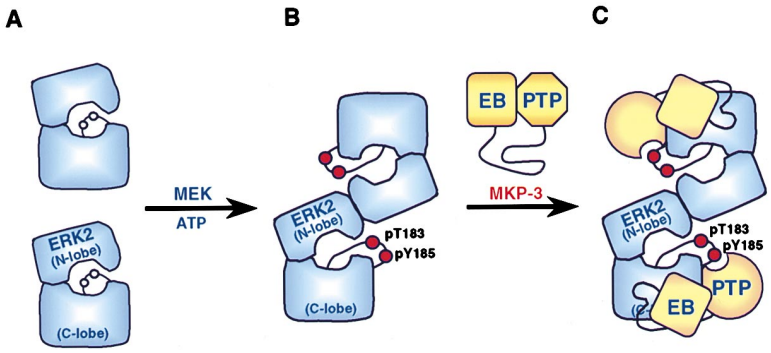

Figure 6. Model for MKP-3 Activation and ERK2 Inactivation

(A) In the unphosphorylated and inactive state, ERK2 exists in a monomeric state.

(B) Upon phosphorylation of the T183 and Y185 residues by an upstream MAPK kinase (MEK), the activated ERK2 undergoes local conformational reconfiguration largely around the activation loop containing the two phosphorylated residues, resulting in homodimerization. ERK2 phosphorylation and homodimerization facilitates its nuclear localization, leading to activation of transcriptional factors and consequently, gene expression.

(C) Upon its expression, MKP-3 exists in the low-activity state, in which its key active site residues in the C-terminal catalytic domain are disengaged for enzymatic catalysis. Binding of the N-terminal EB domain to ERK2 alters intramolecular interactions between the N- and C-terminal domains of MKP-3. This conformational change in MKP-3 allosterically causes a structural rearrangement of the catalytic domain to reconfigure its active site residues to an enzymatically active conformation (high-activity state). The activated MKP-3 then catalyzes dephosphorylation of both phosphorylated T183 and Y185 in ERK2, leading to ERK2 inactivation.

nisms employed in MKP-3 and in the SHP-2 tyrosine phosphatase, which consists of two *Src* homology 2 (SH2) domains and a C-terminal phosphatase domain, shows how divergent structural mechanisms produce related regulatory effects. As shown in the crystal structure (Hof et al., 1998), in the absence of a tyrosine-phosphorylated binding partner, the N-terminal SH2 domain in SHP-2 binds to the phosphatase domain and directly blocks the active site. Thus, the N-SH2 domain acts as a conformational switch by either binding and inhibiting the phosphatase, or binding phosphoproteins and activating the enzyme. The regulation of MKP-3 is achieved by a very different and possibly more complex mechanism of substrate-induced activation. In the absence of the substrate ERK2, the N-terminal EB domain associates with the C-terminal phosphatase domain, which is in the low-activity state due to disengagement of the active site residues. Binding of the EB domain to ERK2 allosterically affects the active site conformation in the phosphatase domain, leading to enzymatic activation of MKP-3. The new three-dimensional structure of the EB domain of MKP-3 represents a first step toward the structural realization of this novel and important regulatory mechanism. The structure reveals the unique features of the β3-α3 region in the conserved Rossmann fold that enable MKP-3 to functionally couple its substrate recognition to substrate-induced upregulation of its phosphatase activity in a cooperative manner. Our results form the foundation for understanding the detailed molecular mechanisms of conformational rearrangements necessary for MKP-3 activation and catalysis of ERK2 dephosphorylation, which will require three-dimensional structures of the full-length MKP-3 protein, both free and in complex with ERK2.

Experimental Procedures

Sample Preparation

Various DNA sequences encoding the MKP-3 EB domain were cloned into a pET15b vector (Novagen), which produces the recombinant protein with a hexahistidine (His_6) sequence at the N terminus. The proteins were overexpressed in *Escherichia coli* BL21(DE3) cells. Uniformly ^{15}N- and $^{15}N/^{13}C$-labeled proteins were prepared by growing bacteria in a minimal medium containing $^{15}NH_4Cl$ with or without $^{13}C_6$-glucose. A uniformly $^{15}N/^{13}C$-labeled and fractionally deuterated protein sample was prepared by using a medium containing 75% ^2H_2O. The EB domain was purified by affinity chromatography on a nickel-IDA column (Invitrogen), followed by the removal of the His_6 tag with thrombin treatment. The cleaved protein was further purified by ion-exchange chromatography. Synthetic peptides were prepared on a MilliGen 9050 peptide synthesizer (Perkin Elmer) with Fmoc/HBTU chemistry. NMR samples contained $\sim$0.5 mM protein in 50 mM imidazole buffer (pH 6.0), 5 mM DTT-d_{10}, 0.5 mM EDTA, 100 mM NaCl, and 200 mM urea in $H_2O/^2H_2O$ (9/1) or ^2H_2O. The low concentration of urea, which did not affect the protein structure as supported by the NMR spectra, was used to stabilize the protein for the NMR structural study. ERK2 protein was expressed and purified by using a procedure described previously (Canagarajah et al., 1997).

NMR Spectroscopy

All NMR spectra were acquired at 25°C on a 600 MHz or 500 MHz Bruker DRX NMR spectrometer. The backbone and side chain ^1H, ^{13}C, and ^{15}N resonances of the protein were assigned deuterium-decoupled triple resonance spectra of HNCA, HN(CO)CA, HNCACB, HN(CO)CACB, and (H)C(CO)NH-TOCSY (Yamazaki et al., 1994; Sattler et al., 1999) recorded on a uniformly $^{15}N/^{13}C$-labeled and fractionally deuterated protein. The side chain assignments were completed with 3D HCCH-TOCSY (Clore and Gronenborn, 1994) data collected from a uniformly $^{15}N/^{13}C$-labeled protein. NOE-derived distance restraints were obtained from ^{15}N- or ^{13}C-edited 3D NOESY spectra (Clore and Gronenborn, 1994). ϕ-angle restraints were determined from $^3J_{HN,H\alpha}$ coupling constants measured in a 3D HNHA-*J* spectrum (Clore and Gronenborn, 1994). Slowly exchanging amide protons were identified from a series of 2D ^{15}N-HSQC spectra recorded after the H_2O buffer was changed to ^2H_2O buffer. All NMR spectra were processed with NMRPipe/NMRDraw (Delaglio et al., 1995) and analyzed by NMRView (Johnson and Blevins, 1994).

^1H and ^{15}N amide resonance changes of the uniformly $^{15}N/^2H$-labeled MKP-3 EB domain were monitored upon the addition of the full-length ERK2 with a series of the sensitivity-enhanced TROSY spectra (Pervushin et al., 1997, 1998).

Structure Calculations

Structures of the MKP-3 EB domain were calculated with a distance geometry–simulated annealing protocol with the X-PLOR program (Brünger, 1993). The initial structure calculations were performed by using manually assigned NOE-derived distance restraints. Hydrogen bond distance restraints were added at the late stage of structural calculations for residues with characteristic NOE patterns. The converged structures were then used for the iterative automated assignment of the NOE spectra by ARIA, which integrates with X-PLOR for structure refinement. The final structure calculations employed a total of 2430 NOE-derived distance restraints obtained from the manual and the ARIA-assisted assignments from the ^{15}N- or ^{13}C-edited NOE data (Nilges and O'Donoghue, 1998; Table 1).

Additionally, 80 hydrogen bond distance restraints for 40 hydrogen bonds and 30 ϕ-angle restraints were also used in the calculations. For the ensemble of the final 20 NMR structures, no distance or torsional angle restraint was violated by more than 0.5 Å or 5°, respectively. The NOE-derived restraints were categorized based on the observed NOE peak intensities.

Mutagenesis and GST Pulldown Assay

Site-directed mutant proteins were prepared with the QuikChange kit (Stratagene). DNA sequencing confirmed the mutations. Effects of mutation of the MKP-3 EB domain on its binding to ERK2 were characterized in a GST pulldown assay. Briefly, GST fusion proteins of the wild-type and various mutants of the EB domain (residues 1–154), the full-length wild-type MKP-3 (residues 1–381), and the MKP-3 active site mutant C293S, as well as GST alone, were incubated overnight at 4°C with an equal amount of ERK2 in the binding buffer, which contained 50 mM Tris (pH 7.5), 0.1 mM EDTA, 1% Triton-100, 10% glycerol, 1 mM PMSF, and 1 mM DTT. The GST protein-bound agarose beads were washed extensively with the binding buffer. The proteins were resolved by SDS-PAGE and analyzed by Western blotting for ERK2 with a monoclonal rabbit anti-ERK2 antibody (Promega) and anti-rabbit IgG antibodies labeled with peroxidase (Promega). The membrane was developed by an enhanced chemiluminescence kit (Amersham).

MKP-3 Phosphatase Activity Assay

Phosphatase activity of MKP-3 was measured as *p*-nitrophenyl phosphate hydrolysis in 1 ml of 50 mM Tris buffer (pH 8.0), containing 5 mM DTT and 10 mM *p*NPP at 22°C in the presence of full-length MKP-3 (0.2 μM) with or without ERK2 (molar ratio 1:1). The reaction was monitored by absorbance at a wavelength of 405 nm. ERK2 binding by various MKP-3 proteins, namely, either the N-terminal MKP-3 fragments or the full-length MKP-3 C293S mutant, was assessed with an inhibition experiment in which reduction of the ERK2-induced activation of MKP-3 phosphatase activity was measured in the presence of these various MKP-3 proteins (1.0 μM).

Acknowledgments

We thank S. Arkinstall and M. Cobb for providing cDNA constructs of MKP-3 and ERK2, respectively. We also thank I. Wolf for peptide synthesis, and M. P. Goldfarb, D. Logothetis, and K. S. Yan for critical reading of the manuscript. A. F. is a recipient of a Wellcome Trust Postdoctoral Fellowship. The work was supported by a grant from the National Institutes of Health (CA80938) to M.-M. Z.

Received August 17, 2000; revised December 7, 2000.

References

Ahn, N.G., Seger, R., Bratlien, R.L., Diltz, C.D., Tonks, N.K., and Krebs, E.G. (1991). Multi components in an epidermal growth factor-stimulated protein kinase cascade. J. Biol. Chem. *266*, 4220–4227.

Brünger, A.T. (1993). X-PLOR Version 3.1: A System for X-Ray Crystallography and NMR, Version 3.1 Edition (New Haven, CT: Yale University Press).

Brunner, D., Oellers, N., Szabad, J., Biggs, W.H., III, Zipursky, S.L., and Hafen, E. (1994). A gain-of-function mutation in *Drosophila* MAP kinase activates multiple receptor tyrosine kinase signaling pathways. Cell *76*, 875–888.

Cahill, M.A., Hanknecht, R., and Nordheim, A. (1996). Signalling pathways: jack of all cascades. Curr. Biol. *6*, 16–19.

Camps, M., Nichols, A., Gillieron, C., Antonsson, B., Muda, M., Chabert, C., Boschert, U., and Arkinstall, S. (1998). Catalytic activation of the phosphatase MKP-3 by ERK2 mitogen-activated protein kinase. Science *280*, 1262–1265.

Canagarajah, B.J., Khokhlatchev, A., Cobb, M.H., and Goldsmith, E.J. (1997). Activation mechanism of the MAP kinase ERK2 by dual phosphorylation. Cell *90*, 859–869.

Cano, E., and Mahadevan, L. (1995). Parallel signal processing among mammalian MAPKs. Trends Biochem. Sci. *20*, 117–122.

Carson, M. (1991). Ribbons 2.0. J. Appl. Cryst. *24*, 958–961.

Chu, Y., Solski, P.A., Khosravi-Far, R., Der, C.J., and Kelly, K. (1996). The mitogen-activated protein kinase phosphatases PAC1, MKP-1, and MKP-2 have unique substrate specificities and reduced activity in vivo toward the ERK2 sevenmaker mutation. J. Biol. Chem. *271*, 6497–6501.

Clarke, P.R. (1994). Switching off MAP kinases. Curr. Biol. *4*, 647–650.

Clore, G.M., and Gronenborn, A.M. (1994). Multidimensional heteronuclear nuclear magnetic resonance of proteins. Methods Enzymol. *239*, 249–363.

Cobb, M.H., and Goldsmith, E. (1995). How MAP kinases are regulated. J. Biol. Chem. *270*, 14843–14846.

Cobb, M.H., and Goldsmith, E.J. (2000). Dimerization in MAP-kinase signaling. Trends Biochem. Sci. *25*, 7–9.

Delaglio, F., Grzesiek, S., Vuister, G.W., Zhu, G., Pfeifer, J., and Bax, A. (1995). NMRPipe: a multidimensional spectral processing system based on UNIX pipes. J. Biomol. NMR *6*, 277–293.

Denu, J.M., and Dixon, J.E. (1995). A catalytic mechanism for the dual-specificity phosphatases. Proc. Natl. Acad. Sci. USA *92*, 5910–5914.

Fjeld, C.C., Rice, A.E., Kim, Y., Gee, K.R., and Denu, J.M. (2000). Mechanistic basis for catalytic activation of mitogen-activated protein kinase phosphatase 3 by extracellular signal-regulated kinase. J. Biol. Chem. *275*, 6749–6757.

Groom, L.A., Sneddon, A.A., Aleesi, D.R., Down, S., and Keyse, S.M. (1996). Differential regulation of the MAP, SAP and RK/p38 kinases by Pyst1, a novel cytosolic dual-specificity phosphatase. EMBO J. *15*, 3621–3632.

Gupta, S., Campbell, D., Derijard, B., and Davis, R.J. (1995). Transcription factor ATF2 regulation by the JNK signal transduction pathway. Science *267*, 389–393.

Gupta, S., Barrett, T., Whitmarsh, A.J., Cavanagh, J., Sluss, H., Derijard, B., and Davis, R. (1996). Selective interaction of JNK protein kinase isoforms with transcription factors. EMBO J. *15*, 2760–2770.

Hof, P., Pluskey, S., Dhe-Paganon, S., Eck, M.J., and Shoelson, S.E. (1998). Crystal structure of the tyrosine phosphatase SHP-2. Cell *92*, 441–450.

Johnson, B.A., and Blevins, R.A. (1994). NMRView: a computer program for the visualization and analysis of NMR data. J. Biomol. NMR *4*, 603–614.

Karin, M. (1995). The regulation of AP-1 activity by mitogen-activated protein kinases. J. Biol. Chem. *270*, 16483–16486.

Keyse, S.M. (1994). An emerging family of dual specificity MAPK kinase phosphatases. Biochim. Biophys. Acta *1265*, 152–160.

Khokhlatchev, A., Xu, S., English, J., Wu, P., Schaefer, E., and Cobb, M.H. (1997). Reconstitution of MAP kinase phosphorylation cascades in bacteria: efficient synthesis of active protein kinases. J. Biol. Chem. *272*, 11057–11062.

Kyriakis, J.M., and Avruch, J. (1996). Sounding and alarm: protein kinase cascades activated by stress and inflammation. J. Biol. Chem. *271*, 24313–24316.

Lewis, T.S., Shapiro, P.S., and Ahn, N.G. (1998). Signal transduction through MAP kinase cascades. Adv. Cancer Res. *74*, 49–139.

Marshall, C.J. (1995). Specificity of receptor tyrosine kinase signaling: transient versus sustained extracellular signal-regulated kinase activation. Cell *80*, 179–185.

Muda, M., Boschert, U., Dickinson, R., Martinou, J.-C., Martinou, I., Camps, M., Schlegel, W., and Arkinstall, S. (1996a). MKP-3, a novel cytosolic protein-tyrosine phosphatase that examplifies a new class of mitogen-activated protein kinase phosphatase. J. Biol. Chem. *271*, 4319–4326.

Muda, M., Theodosiou, A., Rodrigues, N., Boschert, U., Camps, M., Gillieron, C., Davies, K., Ashworth, A., and Arkinstall, S. (1996b). The dual specificity phosphatase M3/6 and MKP-3 are highly selective for inactivation of distinct mitogen-activated protein kinases. J. Biol. Chem. *271*, 27205–27208.

Muda, M., Theodosiou, A., Gilleron, C., Smith, A., Chabert, C., Camps, M., Boschert, U., Rodrigues, N., Davis, K., Ashworth, A., and Arkinstall, S. (1998). The mitogen-activated protein kinase phos-

phatase-3 N-terminal noncatalytic region is responsible for tight substrate binding and enzymatic specificity. J. Biol. Chem. *273*, 9323–9329.

Nilges, M., and O'Donoghue, S. (1998). Ambiguous NOEs and automated NOE assignment. Prog. NMR Spectroscopy *32*, 107–139.

Payne, D.M., Rossomando, A.J., Martino, P., Erickson, A.K., Her, J.-H., Shabanowitz, J., Hunt, D.F., Weber, M.J., and Strurgill, T.W. (1991). Identification of the regulatory phosphorylation sites in pp42/mitogen-activated protein kinases (MAP kinases). EMBO J. *10*, 885–892.

Pervushin, K., Riek, R., Wider, G., and Wüthrich, K. (1997). Attenuated T_2 relaxation by mutual cancellation of dipole-dipole coupling and chemical shift antisotropy indicates an avenue to NMR structures of very large biological macromolecules in solution. Proc. Natl. Acad. Sci. USA *94*, 12366–12371.

Pervushin, K., Wider, G., and Wuthrich, K. (1998). Single transition-to-single transition polarization transfer (ST2-PT) in [^{15}N,^{1}H]-TROSY. J. Biomol. NMR *12*, 345–348.

Richardson, J.S. (1981). The anatomy and taxonomy of protein structure. Adv. Protein Chem. *34*, 167–339.

Robbins, D.J., Zeng, E., Owaki, H., Vanderbilt, C.A., Ebert, D., Geppert, T.D., and Cobb, M.H. (1993). Regulation and properties of extracellular signal-regulated protein kinases 1 and 2 in vitro. J. Biol. Chem. *268*, 5097–5106.

Robinson, M.J., and Cobb, M.H. (1997). Mitogen-activated protein kinase pathways. Curr. Opin. Cell Biol. *9*, 180–186.

Rohan, P.J., Davis, P., Moskaluk, C.A., Kearns, M., Krutzsch, H., Siebenlist, U., and Kelly, K. (1993). PAC-1: a mitogen-induced nuclear protein tyrosine phosphatase. Nature *259*, 1763–1766.

Sattler, M., Schleucher, J., and Griesinger, C. (1999). Heteronuclear multidimensional NMR experiments for the structure determination of proteins in solution employing pulsed field gradients. Prog. NMR Spectroscopy *34*, 93–158.

Sivaraman, V.S., Wang, H.-Y., Nuovo, G.J., and Malbon, C.C. (1997). Hyperexpression of mitogen-activated protein kinase in human breast cancer. J. Clin. Invest. *99*, 1478–1483.

Stewart, A.E., Dowd, S., Keyse, S.K., and McDonald, N.Q. (1999). Crystal structure of the MAPK phosphatase Pyst1 catalytic domain and implications for regulated activation. Nat. Struct. Biol. *6*, 174–181.

Tanoue, T., Adachi, M., Moriguchi, T., and Nishida, E. (2000). A conserved docking motif in MAP kinases common to substrates, activators and regulators. Nat. Cell Biol. *2*, 110–116.

Tonks, N.K., and Neel, B.G. (1996). From form to function: signaling by protein tyrosine phosphatases. Cell *87*, 265–368.

Treisman, R. (1996). Regulation of transcription by MAP kinase cascades. Curr. Opin. Cell Biol. *8*, 205–215.

Wang, X.Z., and Ron, D. (1996). Stress-induced phosphorylation and activation of the transcription factor CHOP (GADD153) by p38 MAP kinase. Science *272*, 1347–1349.

Ward, Y., Gupta, S., Jensen, P., Wartmann, M., Davis, R.J., and Kelly, K. (1994). Control of MAP kinase activation by the mitogen-induced threonine/tyrosine phosphatase PAC1. Nature *367*, 651–654.

Waskiewicz, A.J., and Cooper, J.A. (1995). Mitogen and stress response pathways: MAP kinase cascades and phosphatase regulation in mammals and yeast. Curr. Opin. Cell Biol. *7*, 798–805.

Whitmarsh, A.J., Shore, P., Sharrocks, A.D., and Davis, R.J. (1995). Integration of MAP kinase signal transduction pathways at the serum response element. Science *269*, 403–407.

Yamazaki, T., Lee, W., Arrowsmith, C.H., Mahandiram, D.R., and Kay, L.E. (1994). A suite of triple resonance NMR experiments for the backbone assignment of ^{15}N, ^{13}C, ^{2}H labeled proteins with high sensitivity. J. Am. Chem. Soc. *116*, 11655–11666.

Zhou, B., and Zhang, Z.-Y. (1999). Mechanism of mitogen-activated protein kinase phosphatase-3 activation by ERK2. J. Biol. Chem. *274*, 35526–35534.

Protein Data Bank ID Code

The MKP-3 EB domain structure has been deposited in the Protein Data Bank under the ID code 1HZM.